Accepted Manuscript

Enhanced shape selective catalysis of mixed cyclic ketones in aerobic Baeyer-Villiger oxidation with magnetic Cu-Fe$_3$O$_4$ supported mesoporous silica microspheres

Chunming Zheng, Shubin Chang, Chuanwu Yang, Dongying Lian, Chao Ma, Chunrong Zhang, Xiangrui Fan, Shichao Xu, Xiaohong Sun

Enhanced shape selective catalysis of mixed cyclic ketones in aerobic Baeyer-Villiger oxidation with magnetic Cu-Fe$_3$O$_4$ supported mesoporous silica microspheres

Chunming Zheng[a,*], Shubin Chang[a], Chuanwu Yang[a], Dongying Lian[a], Chao Ma[a], Chunrong Zhang[a], Xiangrui Fan[a], Shichao Xu[a], Xiaohong Sun[b,*]

ChunMing Zheng, State Key Laboratory of Separation Membranes and Membrane Processes, School of Environmental and Chemical Engineering, Tianjin Polytechnic University, Tianjin 300387, P.R. China, zhengchunming@tjpu.edu.cn Tel.: +86 022 83955661

ShuBin Chang, School of Environmental and Chemical Engineering, Tianjin Polytechnic University, Tianjin 300387, P.R. China, 1472451963@qq.com Tel.: +86 022 83955661

ChuanWu Yang, School of Environmental and Chemical Engineering, Tianjin Polytechnic University, Tianjin 300387, P.R. China, 1558862045@qq.com Tel.: +86 022 83955661

DongYing Lian, School of Environmental and Chemical Engineering, Tianjin Polytechnic University, Tianjin 300387, P.R. China, 1761713372@qq.com Tel.: +86 022 83955661

Chaos Ma, School of Environmental and Chemical Engineering, Tianjin Polytechnic University, Tianjin 300387, P.R. China, 1325249973@qq.com Tel.: +86 022 83955661
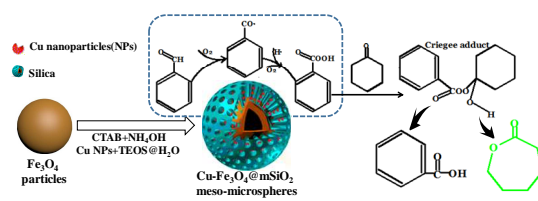
Chunrong Zhang, School of Environmental and Chemical Engineering, Tianjin Polytechnic University, Tianjin 300387, P.R. China, 2770158793@qq.com Tel.: +86 022 83955661

Xiangrui Fan, School of Environmental and Chemical Engineering, Tianjin Polytechnic University, Tianjin 300387, P.R. China, 1223220075@qq.com Tel.: +86 022 83955661

ShiChao Xu, School of Environmental and Chemical Engineering, Tianjin Polytechnic University, Tianjin 300387, P.R. China, xushichao_tj@126.com Tel.: +86 022 83955661

Xiaohong Sun, Key Laboratory of Advanced Ceramics and Machining Technology, Ministry of Education, School of Materials Science and Engineering, Tianjin University, Tianjin 300072, P.R. China, sunxh@tju.edu.cn Tel.: +86 022 27406114

Graphical Abstract

Enhanced shape selective catalysis of mixed cyclic ketones in aerobic Baeyer-Villiger oxidation with magnetic Cu-Fe₃O₄ supported mesoporous silica microspheres

Chunming Zheng[a,*], Shubin Chang[a], Chuanwu Yang[a], Dongying Lian[a], Chao Ma[a], Chunrong Zhang[a], Xiangrui Fan[a], Shichao Xu[a], Xiaohong Sun[b,*]

a State Key Laboratory of Separation Membranes and Membrane Processes, School of Environmental and Chemical Engineering, Tianjin Polytechnic University, Tianjin 300387, China.

b Key Laboratory of Advanced Ceramics and Machining Technology, Ministry of Education, School of Materials Science and Engineering, Tianjin University, Tianjin 300072, China.

* Corresponding author. Tel.: +86 022 83955661; fax: +86 022 83955140.

E-mail address: zhengchunming@tjpu.edu.cn (C.M. Zheng).

* Corresponding author. Tel.: +86 022 27406141; fax: +86 022 27406114.

E-mail address: sunxh@tju.edu.cn (X.H. Sun).

Abstract

Various strategies have been developed to improve the conversion for the Baeyer-Villiger oxidation. However, the catalytic effects of the Baeyer-Villiger oxidation for the mixed ketones are rarely reported, though it is also important for the natural and industrial separation processes. In this report, magnetite Cu modified Fe_3O_4 supported mesoporous silica microspheres ($Cu-Fe_3O_4@mSiO_2$) have been successfully synthesized by two step direct hydrothermal method (DHT). Over 99 % of cyclohexanone conversion was obtained with mild air oxidation and benzaldehyde as sacrificing agent over $Cu-Fe_3O_4@mSiO_2$. The catalytic system also shows higher conversion rates for small molecular ketones in the mixed ketone reactants, which was attributed to the enhanced mass transfer effect and Fe-Cu composite active sites in the magnetite mesoporous silica microspheres. The catalyst could be recycled for four times with similar catalytic performance, which shows enhanced shape selectivity in aerobic Baeyer-Villiger oxidations for mixed cyclic ketones.

Key words: magnetite mesoporous silica microspheres; Baeyer-Villiger oxidation; copper; enhanced shape selectivity

1. Introduction

Baeyer-Villiger (B-V) oxidation is a valuable organic reaction, which could provide a direct pathway to convert ketones to corresponding lactones or esters [1-4]. However, organic peracids as traditional oxidants has many disadvantages such as high cost, low selectivity and environmental hazards [5-10]. Therefore, developing high efficient and green oxidants is an important issue. According to these reports, molecular oxygen and H_2O_2 as environmental-friendly oxidants have been successfully carried out for B-V oxidation using different catalysts like graphite [11,12], Cu-MCM-41 [13], Ketjen Black [14], Sn-MFI nanosheets and Sn-Beta zeolites [15,16]. The O_2/aldehydes system for B-V oxidation is an important method, which could avoid using explosive peracetic acid, corrosive hydroperoxides and expensive protection. However, in the O_2/aldehydes oxidation system, large amounts of aldehydes over stoichiometric ratio (e.g., 3 equiv.) were required as sacrificing agents for the oxidation of cyclohexanone, resulting in large amounts of benzoic acid. Moreover, in practical applications, the oxidation of ketones often has some complicated mixed systems, which also reduced the oxidation and selectivity of ketones. Meanwhile, the system suffered from the limitation of complicated synthesis of catalysts [17, 18], relatively low activity, longer reaction time and much consumption of aldehydes [19, 20]. If the efficiency of sacrificing agent becomes higher and the selectivity of the catalyst was better, the catalytic system would be better applied to practical applications, which plays important shape selective catalytic effect and become more environmental friendly and fascinating.

3

In recent years, core-shell magnetic mesoporous silica nanoparticles have been subjected to extensive research for the combined functionalities of magnetism and mesoporous nanostructures. With their unique and strong magnetic responsivity, high chemical stability, enhanced metal oxides dispersion and recoverability, magnetic microspheres have shown great application potentials in many research fields, such as bioseparation [21], enrichment [22], enzyme immobilization [23], adsorption and catalysis [24-26]. What is more, because of its high reduction potential and redox property, copper is also widely used as high efficient metal catalytic component for the oxidation reactions of hydrocarbon compounds, such as alcohol [27], aniline compounds [28], especially for B-V oxidation of various ketones [13, 29, 30]. The redox reaction of iron ions with copper was speed up for the increased rate of transferring the electrons on the silicon-based catalysts. Meanwhile, the catalysts activities were also promoted by the excellent electron transfer ability of catalyst. Therefore, it motivated us to explore and design the catalysts consisting of Fe-Cu composite metal oxides for the aerobic B-V oxidation.

Herein, in this work, magnetic Cu modified Fe_3O_4 supported mesoporous silica microspheres (Cu-Fe_3O_4@mSiO_2, core-shell) was fabricated for aerobic Baeyer-Villiger oxidation of cyclic ketones with benzaldehyde. Cu-Fe_3O_4@mSiO_2 converts mixed cyclic ketones to corresponding lactone under relatively mild conditions with high activity and differential selectivity. The mechanism for different catalytic activity and selectivity of composite Cu-Fe_3O_4 metallic center was also investigated with N_2 sorption, XRD, UV-vis, FT-IR, TEM and VSM characterizations.

4

2. Results and discussion
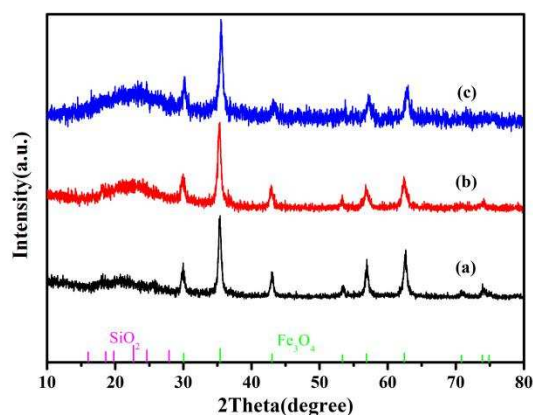
2.1. Catalyst characterizations

Fig. 1. Large angle XRD patterns of synthesized Fe_3O_4 (a), $Fe_3O_4@mSiO_2$ (b) and

$Cu-Fe_3O_4@mSiO_2$ (c).

In order to characterize the porous structure of synthesized catalysts, large-angle

XRD patterns of synthesized Fe_3O_4, $Fe_3O_4@mSiO_2$ and $Cu-Fe_3O_4@mSiO_2$ were

investigated and shown in Fig. 1. The typical characteristic diffraction peaks matched

with the standard Fe_3O_4 reflections (JCPDS 89-0688, green standard peak), which

suggests the Fe_3O_4 particles are well retained in all prepared processes with well

crystalline and pure phase. From Fig. 1, there is a broad peak around 22º, which is due

to the presence of amorphous porous SiO_2 (JCPDS 82-1571, main standard peak),

implying the porous silica has been successfully coated on the surface of Fe_3O_4

particles. With the modification of Cu on $Fe_3O_4@mSiO_2$ and the subsequent

calcination of the catalyst at 550 °C for 6 h, the diffraction peaks of $Cu-Fe_3O_4@mSiO_2$

5

at 30.175°, 35.543°, 43.199°, 57.135°, 62.744° could be indexed to the (111), (220), (311), (400), (511) and (440) planes of $CuFe_2O_4$ crystal (JCPDS 77-0010), which implied the iron and copper species react strongly and combine together to formed a new phase. Meanwhile, the diffraction peak of SiO_2 increases which indicates the high SiO_2 content and purities in the sample [31]. This conclusion could be further evidenced by the following TEM characterization. The small XRD characterization was not shown since there was no obvious peak in 0~5°, which might due to the mesoporous structure of SiO_2 was not highly ordered.

Fig. 2 shows the TEM images of synthesized Fe_3O_4 particles, $Fe_3O_4@mSiO_2$ microspheres and $Cu-Fe_3O_4@mSiO_2$ microspheres. From Fig.2a, the magnetite Fe_3O_4 particles are uniformly synthesized both in morphology and size, which have a mean diameter of about 300 nm. In Fig. 2b, the $Fe_3O_4@mSiO_2$ microspheres have a core-cell nanoparticle texture with thin silica layer of ~20 nm in thickness according to the difference between core and shell, demonstrating the Fe_3O_4 nanoparticles have been successfully coated by porous silica shell. As shown in Fig.2c, the TEM images exhibits Cu modified Fe_3O_4 supported mesoporous silica microspheres core-shell structure. The porous silica layer in the outer layer was about ~20 nm in thickness[25]. Notably, the shape and texture of $Cu-Fe_3O_4@mSiO_2$ microspheres nearly remain unchanged after calcination in tube furnace at 550 °C in air for 6 h. The surface roughness of the material slightly increased, which suggested the isolated introduction of Cu^{2+} into the material did not change the structure of $Cu-Fe_3O_4@mSiO_2$ microspheres.
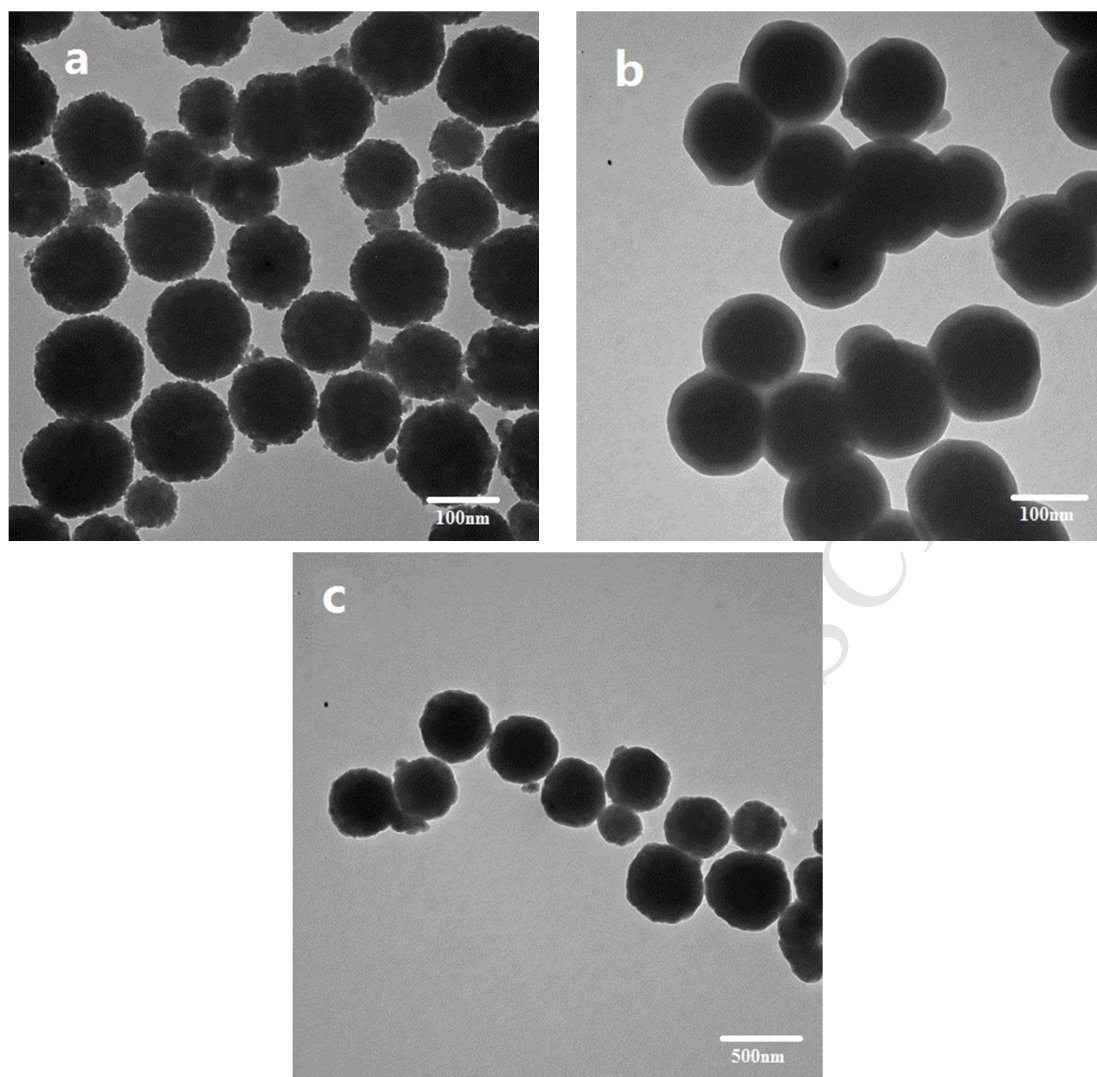
6

Fig. 2. TEM images of synthesized Fe_3O_4 particles (a), Fe_3O_4@$mSiO_2$ (b) and

Cu-Fe_3O_4@$mSiO_2$ microspheres (c).

Fig. 3 shows N_2 adsorption-desorption isotherms and the corresponding

mesoporous size distribution of the synthesized Cu-Fe_3O_4@$mSiO_2$ (20) microspheres.

From Fig. 3a, N_2 adsorption isotherms of IV-type curves could be observed with a H_2

hysteresis loop, which is typical for mesoporous materials. Fig. 3b shows the catalyst

has a sharp peak centered at average pore size of 2.5 nm, indicating the mesoporous

structure of the catalyst. The BET surface area and the total pore volume are 405 m^2/g

and 0.30 cm^3/g, respectively. According to above analysis, it reflects the incorporation of copper into the framework cannot change the uniform hollow micro-mesoporous structure of the Fe$_3$O$_4$@mSiO$_2$, which could benefit the selectivity for the small molecular ketones in the mixed cyclic ketones [26].

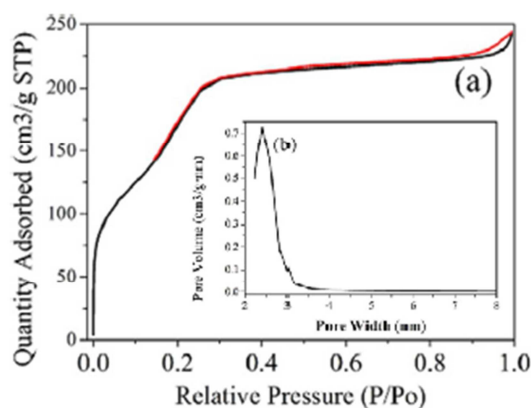**Fig. 3.** N$_2$ adsorption-desorption isotherms of Cu-Fe$_3$O$_4$@mSiO$_2$ (20) microspheres (a) and the corresponding mesoporous diameter distribution (b).

Fig. 4 shows the FT-IR spectra of Cu-Fe$_3$O$_4$@mSiO$_2$ with different Si/Cu ratio in the range of 500 ~ 1500 cm^{-1}. The bands at around 1080 cm^{-1} and 800 cm^{-1} were distinct for all the catalysts and attributed to the asymmetric stretching vibration and symmetric stretching vibration mode of Si-O-Si bridges, respectively [30]. The band at around 960 cm^{-1} is related with Si-O-Cu vibration and has been interpreted according to the literature [32]. Meanwhile, the peak is also widely regarded as the characterization peak for the transition metal ions in the silica framework. With the Cu content increasing, the intensity of the band at around 960 cm^{-1} also increased. These results imply the Cu element has been incorporated in the Fe$_3$O$_4$@mSiO$_2$ framework and the

8

catalysts activities for cyclic ketones could also be promoted with the redox reaction

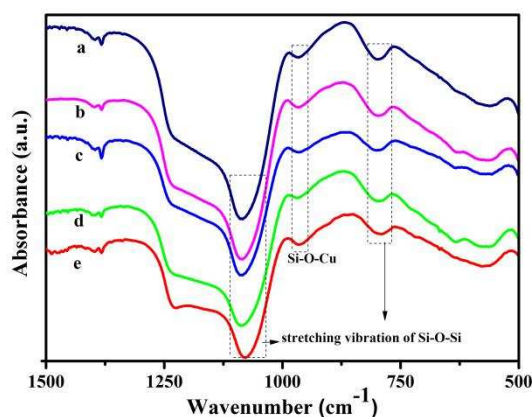and the cooperated electron transfer ability of Fe-Cu composite metal oxides.

Fig. 4. FT-IR spectra of $Fe_3O_4@mSiO_2$ (e) and $Cu-Fe_3O_4@mSiO_2$ with different

Si/Cu ratio at 20:1 (a); 50:1 (b); 100:1 (c); 200:1 (d), responding to Fe/Cu ratio (20:1,

40:1, 80:1; 160:1).

Fig. 5 shows the magnified hysteresis loops of Fe_3O_4 (a), $Fe_3O_4@mSiO_2$ (b) and

$Cu-Fe_3O_4@mSiO_2$ (c), which also clearly indicates that no remanence are detected,

reflecting the superparamagnetic property. The saturation magnetization value of

Fe_3O_4 is 73.88 emu/g. After coated with a layer of porous silica, the magnetization

value of Fe_3O_4 is measured to 58.49 emu/g, then further decreases to 17.31 emu/g

after coated with the layer of mesoporous silica and the introduction of Cu^{2+} ions. The

decrease in magnetizing saturation is attributed to the presence of nonmagnetic SiO_2,

mesoporous silica and some copper nanoparticles inside the uniformly pore of hollow

mesoporous spheres. The mesoporous silica microspheres have high magnetite

contents and good magnetic responsivity, beneficial to a fast and efficient separation

9

with the aid of an external magnetic field and purification processes. As shown in the internal figure of Fig. 5., the mixed particles could be completely separated by external magnet, suggesting the magnetic and easy separation properties of mixed particles.
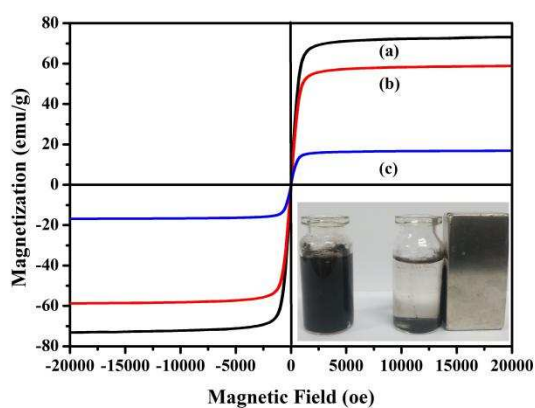

Fig. 5. Magnified hysteresis loops of different samples at room temperature: Fe_3O_4 (a), $Fe_3O_4@mSiO_2$ (b), $Cu-Fe_3O_4@mSiO_2$ (c).

In order to investigate the coordination form of Cu species, the UV-Vis spectra of $Cu-Fe_3O_4@mSiO_2$ with different Si/Cu ratio were measured spanning from 200 nm ~ 800 nm (Fig. 6). All the catalysts showed a shoulder adsorption peak centering around at 250 nm, which could be assigned to the ligand-to-metal charge transfer between isolated Cu^{2+} and the oxygen of SiO_2 [28,33]. From Fig. 6, the shoulder adsorption peak also indicates the retention of Cu^{2+} in octahedral coordination. And the intensity of this band increases proportionally with the addition of Cu^{2+} loading, especially for $Cu-Fe_3O_4@mSiO_2$ (20) and $Cu-Fe_3O_4@mSiO_2$ (50), which suggests more mononuclear Cu^{2+} were supported into mesoporous silica matrix with magnetic

10

nucleus. In addition, the weak and broad bands between 400 and 600 nm in the catalysts with different Si/Cu ratio suggests linear oligonuclear clusters inserted into mesoporous channel. Furthermore, there is a shoulder peak between 600 and 800 nm, which might indicate the formation of bulky CuO particles [33]. Recently, the catalytic efficiency of several iron- and copper-based BV catalysts could be improved since the redox properties of dissolved transition metal cations (Fe^{2+}, Cu^{2+}) allow generating highly active hydroxyl radicals in the aerobic oxidative condition. Rahman et al. synthesized high surface area mesoporous M-Co-HMS-X (metal = Ni, Fe, Cu). Efficient catalyst with high catalytic activity (>99% cyclohexanone conversion and >99% epsilon-caprolactone selectivity) for the oxidation of cyclohexanone to epsilon-caprolactone could be observed, which might due to the cooperative role of cobalt and iron towards catalytic activity [30]. Wang et al. also synthesized Fe-Cu bimetal oxides with benzaldehyde and air as complex oxidant. The addition of Fe could not only improve the catalytic activity, but also increase the recycling batch performance. But the selectivity issue was not mainly discussed in the report [35].
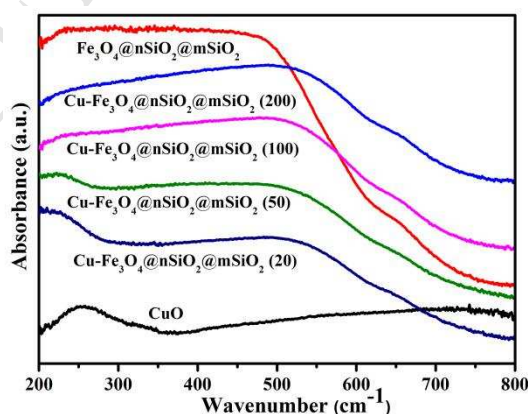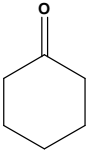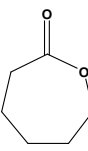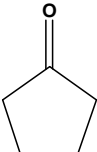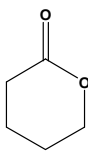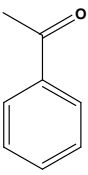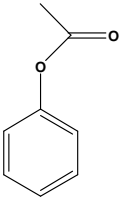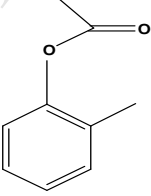

Fig. 6. UV-vis spectra of Cu-Fe$_3$O$_4$@mSiO$_2$ with different Si/Cu ratio (20:1; 50:1;

100:1; 200:1).

11

2.2. Catalytic performance of materials

Table 1 shows the results of catalytic performance towards B-V oxidation of different ketones. Based on above results, all cyclic ketones could be converted to the corresponding lactones with excellent selectivity (>99.0 %) under mild reaction conditions. Cyclohexanone is easier than cyclopentanone to be converted to corresponding lactone in consistent with other reports (entries 1 ~ 2) [12]. In addition, acetophenones with a methyl group have higher conversion than acetophenone without it (entries 3 ~ 5), which is related to the methyl group fixed the positive charge [16]. Meanwhile, the steric-hindrance effect of substituent in six-membered cyclic ketones has an important influence on the conversion of cyclic ketones (entries 4 ~ 5). The B-V conversion of *p*-methyl acetophenone is higher than *o*-methyl acetophenone. For the mesoporous structure of Cu-Fe$_3$O$_4$@mSiO$_2$, it can be 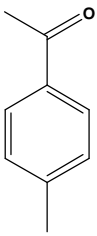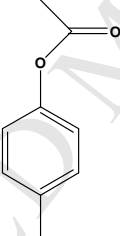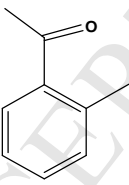due to the chemical structure of ketones which gives rise to the steric hindrance [36]. In addition, same mole of cyclohexanone, cyclopentanone, acetophenone, 4-methylacetophenone and 2-methylacetophenone mixed together were oxidized according to the same reaction conditions (entry ~ 6), the conversion of cyclohexanone is higher than that of the other four substances, which could be deduced the mesoporous structure of Cu-Fe$_3$O$_4$@mSiO$_2$ has certain shape-selectivity for mixed cyclic ketones.

Table 1 The BV oxidation reaction of various ketones with Cu-Fe$_3$O$_4$@mSiO$_2$ as

catalyst.[a]

Entry	Substrate	Product	Conv. [b](%)		Sel. [c](%)
1			>99.0		>99.0
2			75.1		>99.0
3			10.0		>99.0
4			55.7		>99.0
5			50.3		>99.0
6[d]	Mixed Ketones 1 ~ 5	Mixed Esters 1 ~ 5	1	80.0	>99.0
			2	59.7	>99.0
			3	33.0	>99.0
			4	34.4	>99.0
			5	30.6	>99.0

13

The mass transfer of the ketones with large molecular weight was reduced to the active group on the catalysts surface, which might be due to the increased transfer resistance for the molecular size and finite mesoporous structures of Cu-Fe$_3$O$_4$@mSiO$_2$. Hence, their activity is relatively lower for these ketones under the same conditions [27, 29]. With further modification of outer surface Fe-Cu composite active sites, the shape-selectivity of Cu-Fe$_3$O$_4$@mSiO$_2$ might be further precisely controlled [30, 31].

Table 2 shows the catalytic activities of silica materials with different molar ratio of Si to Cu for the Baeyer-Villiger oxidation, which was tested in the presence of benzaldehyde as sacrificing agent and air (20 mL/min). For all the cases, the selectivity of ε-caprolactone reached 99.0 % based on the internal standard method. For Fe$_3$O$_4$@mSiO$_2$, the conversion of cyclohexanone and benzaldehyde were 27.3 % and 29.6 %, separately, which was similar to the effect of the blank reaction though it has got quite high surface area. However, copper doped Fe$_3$O$_4$@mSiO$_2$ showed increased catalytic performance towards B-V oxidation than that of Fe$_3$O$_4$@mSiO$_2$ with the increasing content of Cu to the catalysts. When the molar ratio of Si to Cu

was 20, the cyclohexanone and the benzaldehyde conversion reached 99.0 % and 92.0 %, respectively (table 2, entries 3 ~ 6).

Table 2 Catalytic results of Baeyer-Villiger oxidation of cyclohexanone using

$Cu-Fe_3O_4@mSiO_2$ catalysts with different molar ratio of Si to Cu.[a]

Entry	Catalysts	Conv.[b](%)	Sel.[c](%)	Conv.[d](%)
1	Blank	33.0	>99.0	20.8
2	$Fe_3O_4@mSiO_2$	27.3	>99.0	29.6
3	$Cu-Fe_3O_4@mSiO_2(20)$	>99.0	>99.0	92.0
4	$Cu-Fe_3O_4@mSiO_2(50)$	96.8	>99.0	82.3
5	$Cu-Fe_3O_4@mSiO_2(100)$	82.8	>99.0	74.6
6	$Cu-Fe_3O_4@mSiO_2(200)$	63.7	>99.0	60.0
7	$I-Cu-Fe_3O_4@mSiO_2(20)$	90.0	>99.0	89.7

[a] Reaction conditions: the catalysts (50 mg), DCE (10 mL), cyclohexanone (2 mmol, 206 uL), benzaldehyde (4 mmol, 405 uL), air (20 mL/min), 50 °C, reaction time 6 h. [b] Conversion of cyclohexanone based on GC analysis. [c] Selectivity of ε-caprolactone. [d] Conversion of benzaldehyde. The dodecane used as an internal standard.

According to the characterizations of UV-Vis and FT-IR, the increasing of catalytic activities was matched with the rising of isolated Cu^{2+} content in the catalysts. Since the Cu element had varied valences, the synergetic effect of Cu and Fe redox properties both existed on the surface of catalyst. And the redox reaction of iron ions with copper was speed up for the increased rate of transferring the electrons on the

15

silicon-based catalysts [37]. Meanwhile, the catalysts activities were also promoted by the excellent electron transfer ability of Cu-Fe$_3$O$_4$@mSiO$_2$ catalyst [38]. Therefore, the isolated Cu^{2+} as Lewis acid could be the active sites in the aerobic B-V oxidation and could activate benzaldehyde and cyclohexanone [13, 34]. Furthermore, the oxidant efficiency of benzaldehyde gradually increased with the content of copper in the Fe$_3$O$_4$@mSiO$_2$ (Table 2, entries 3 ~ 6). The reason may rely to the influence of isolated Cu^{2+} species and the improved oxidant efficiency with the addition of benzaldehyde and air. On the basis of above experiment results and analysis, Cu-Fe$_3$O$_4$@mSiO$_2$ (20) was chosen as the catalyst to explore the B-V catalytic oxidation in the following experiments.

Table 3 Effect of different solvents on the conversion of cyclohexanone with Cu-Fe$_3$O$_4$@mSiO$_2$ as catalyst.[a]

Entry	Solvent	Conv.[b](%)	Sel.[c](%)	Conv.[d](%)
1	DCE	>99.0	>99.0	92.0
2	MeCN	72.58	>99.0	88.98
3	DIOX	5.29	>99.0	11.05
4	THF	7.35	>99.0	8.85
5	DMSO	Traces	/	Traces

[a] Reaction conditions: the catalysts (50 mg), solvent (10 mL), cyclohexanone (2 mmol, 206 uL), benzaldehyde (4 mmol, 405 uL), air (20 mL/min), 50 °C, reaction time 6 h. [b] Conversion of

cyclohexanone based on GC analysis. [c] Selectivity of ε-caprolactone. [d] Conversion of benzaldehyde. The dodecane as an internal standard.

In order to investigate the effect of different solvents on the B-V oxidation reaction, Table 3 summarized the results of several solvents on the effect of B-V oxidation of cyclohexanone to ε-caprolactone. From Table 3, the solvent was not a neglected factor in the B-V reaction. Among several solvents investigated, the nonpolar solvent like 1,2-dichloroethane (DCE) gave much higher conversion of cyclohexanone and benzaldehyde than that of other polar solvents, e.g. acetonitrile (MeCN), 1,4-dioxane (DIOX). Furthermore, tetrahydrofuran (THF) and dimethylsulfoxide (DMSO) as solvents would give poor performance in cyclohexanone and benzaldehyde conversion.

Table 4 The effect of different aldehydes on the catalytic activity of aerobic B-V oxidation of cyclohexanone with Cu-Fe$_3$O$_4$@mSiO$_2$ as catalyst.[a]

Entry	Aldehyde	Conv.[b](%)	Yield.[c](%)	Sel.[d](%)
1	None	0	0	0
2	Benzaldehyde	>99.0	>99.0	>99.9
3	Propanal	94.4	94.4	>99.9
4	2,3-Dichlorobenzaldehyde	59.3	59.3	>99.9
5	p-Tolualdehyde	50.2	50.2	>99.9
6	p-Anisaldehyde	11.6	11.6	>99.9

Therefore, 1,2-dichloroethane was the most suitable solvent for B-V oxidation reaction of cyclohexanone. And the solvents of the reaction system proved to have great influence for the aerobic B-V oxidation of cyclic ketones.

Table 4 summarized the cyclohexanone oxidation over Cu-Fe$_3$O$_4$@mSiO$_2$ with different aldehydes as sacrificing agents. For benzaldehyde as sacrificing agent, the B-V oxidation of cyclohexanone gave higher conversion (99.0 %) and selectivity (99.0 %) in the tested aldehydes. Meanwhile, the straight-chain aldehydes could perform as a better sacrificing agent than these aldehydes with branched-chain, which showed better performance in the aerobic B-V oxidation (Table 4, entries 2 ~ 6). The reason may lie to straight-chain aldehydes were favorable to generate more free radicals as a result of the resonance effect [30]. The benzaldehyde with an electron-withdrawing group gave higher conversion than the benzaldehyde with electron-donating group for aerobic B-V oxidation. Furthermore, when there is no aldehyde in the reaction, the poor performance and no reaction occurred for the BV oxidation. Therefore, aldehyde also played an important role in the aerobic B-V oxidation system, which was mentioned by the former investigation [34].

18

2.3. Recycling studies

In order to estimate the stability and reusability of Cu-Fe$_3$O$_4$@mSiO$_2$ for practical application, the recycling tests were also investigated (Fig. 7). To compare the changes of the catalytic performance before and after the reaction, the catalyst amount and reaction time of Cu-Fe$_3$O$_4$@mSiO$_2$ were reduced to 20 mg and 4 h, which the steady and low conversion rates (about 25 %) could be obtained and shown after 5 consecutive runs. Under the high reaction rate, the real catalytic activity of mesoporous Cu-Fe$_3$O$_4$@mSiO$_2$ could not be obtained since the rate determining processes are not only depended on the catalysts performance but also on the reactant supply. From Fig. 7, the similar conversion of cyclohexanone and benzaldehyde remains after the five consecutive runs, which means mesoporous Cu-Fe$_3$O$_4$@mSiO$_2$ catalyst could be reused without remarkable loss in the catalytic performance during the B-V oxidation processes. Hence, Cu-Fe$_3$O$_4$@mSiO$_2$ could be a high efficient and recyclable catalyst in the cyclohexanone B-V oxidation.
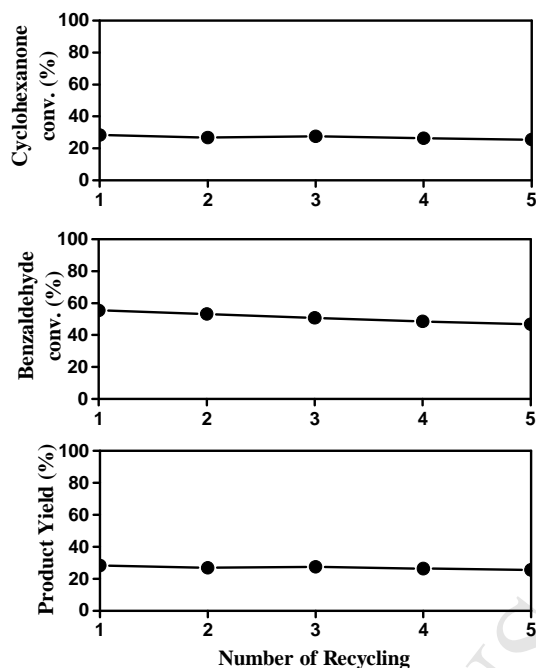
Fig. 7. Reusability of the recovered Cu-Fe_3O_4@$mSiO_2$ in the B-V oxidation of

cyclohexanone. Reaction conditions: the catalysts (20 mg), DCE (10 mL),

cyclohexanone (2 mmol, 206 uL), benzaldehyde (4 mmol, 405 uL), air (10

mL/min), 50 °C, reaction time 4 h.

2.4. Reaction mechanism

Based on above investigation, the catalytic mechanism of Cu-Fe_3O_4@$mSiO_2$ for the

oxidation of cyclohexanone could be proposed. According to literature, the main two

reaction steps of cyclohexanone oxidation with O_2/aldehyde includes (a) peracid

formation from aldehyde and O_2 and (b) peracid oxidation of the cyclohexanone [14].

Nabae et al. found the Ketjen Black carbon could convert cyclohexanone to

ε-caprolactone without metal active sites in O_2/aldehyde condition and proposed the

carbon materials is responsible for the formation of peracid from O_2 and aldehyde

(step (a)) but not for the ketone oxidation (step (b)). It is also meaningful to know

20

which reaction step is enhanced by the Cu-Fe$_3$O$_4$@mSiO$_2$. Therefore, m-cholorobenzaldehyde was used as catalytic performance test in the step (a) and characterized with FT-IR to analyze the residue after the solvent was removed. From FT-IR results shown in Fig.8, in the sample (a), the m-chlorobenzoic acid was generated from m-cholorobenzaldehyde since characteristic peaks of m-chlorobenzoic acid exists at 2100-3300 cm^{-1} (the broadband of O-H stretch and H-bonded) and 1719 cm^{-1} (C=O stretch). Compared with the sample (b), it could be confirmed that no m-choloroperoxybenzoic acid generated without Cu-Fe$_3$O$_4$@mSiO$_2$. For the generated spectrum with Cu-Fe$_3$O$_4$@mSiO$_2$ became complicated, sample (b) seemed a kind of mixture. To confirm the presence of peroxybenzoic acid, sample (b) was washed with sodium bicarbonate solution to remove the benzoic acid and then recrystallized using dichloromethane and hexane solution [14,15]. The spectrum of this purified sample (c) showed several characteristic peaks of about 3500 cm^{-1} (O-H stretch) and 1756 cm^{-1} (C=O stretch) which confirms the presence of m-chloroperoxybenzoic acid. Therefore, the peracid generation was confirmed during the O$_2$/aldehyde B-V oxidation in Cu-Fe$_3$O$_4$@mSiO$_2$ catalytic system. No m-chloroperoxybenzoic acid was observed with the same purification procedure to the sample (a) which suggested Cu-Fe$_3$O$_4$@mSiO$_2$ microspheres could catalyze the formation of peracid from O$_2$ and aldehyde.

21
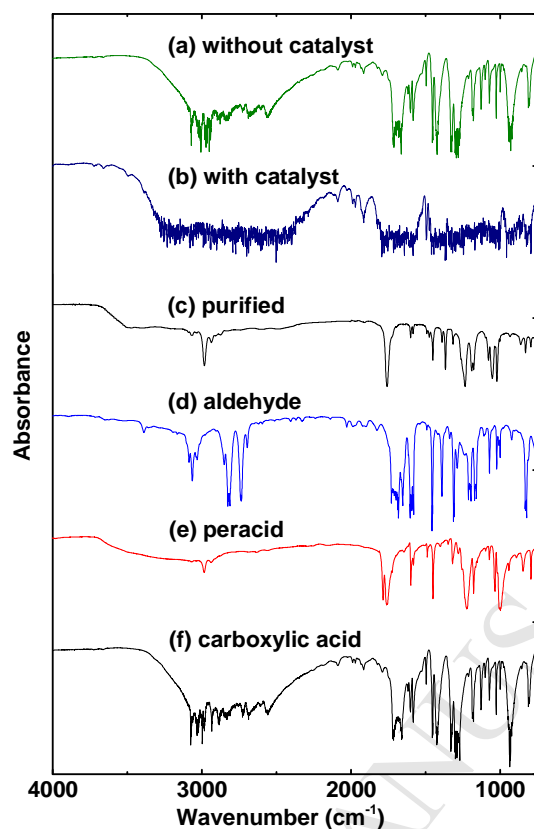
Fig. 8 FT-IR spectra of (a) m-chlorobenzaldehyde treated without catalyst, (b) m-chlorobenzaldehyde treated with Cu-Fe$_3$O$_4$@mSiO$_2$, (c) purified sample from sample b, (d) m-chlorobenzaldehyde, (e) m-chloroperoxybenzoic acid and (f) m-chlorobenzoic acid. Reaction conditions: the catalysts (50 mg), DCE (10 mL), m-cholorbenzaldehyde (4 mmol), air (20 mL/min), 50 °C, reaction time 6 h.

For the step (b), in order to confirm whether Cu-Fe$_3$O$_4$@mSiO$_2$ could accelerate the oxidation of cyclohexanone in the presence of peracid, the oxidation of cyclohexanone by m-chloroperoxybenzoic acid was performed with and without the Cu-Fe$_3$O$_4$@mSiO$_2$ catalyst. From the results summarized in the Table 5, the conversion and selectivity of the O$_2$/aldehyde B-V oxidation remained similar with and without the Cu-Fe$_3$O$_4$@mSiO$_2$, which showed the Cu-Fe$_3$O$_4$@mSiO$_2$ did not

catalyze the cyclohexanone B-V oxidation once peracid generated in the reaction. From above results, it clearly suggested the Cu-Fe$_3$O$_4$@mSiO$_2$ catalyst were only responsible for the generation of m-chloroperoxybenzoic acid and did not contribute to the ketone oxidation for step (b).

Table 5 Cyclohexanone oxidation by m-chloroperoxybenzoic acid.[a]

Catalyst	Conv.[b](%)	Yield.[c](%)	Sel.[d](%)
Cu-Fe$_3$O$_4$@mSiO$_2$	44	44	>99
no catalyst	41	41	>99

[a] Reaction conditions: the catalysts (20 mg), DCE (10 mL), cyclohexanone (2 mmol, 206 uL), m-chloroperoxybenzoic acid (4 mmol), air (10 mL/min), 50 °C, reaction time 4 h. [b] Conversion of cyclohexanone based on GC analysis. [c] Yield of ε-caprolactone. [d] Selectivity of ε-caprolactone. The dodecane used as an internal standard.
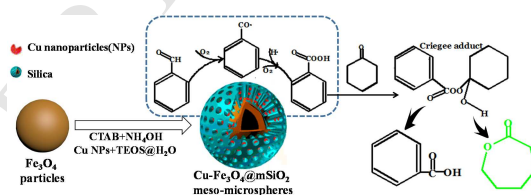
Scheme 1. Possible reaction pathways involved in the B-V oxidation of cyclohexanone with Cu-Fe$_3$O$_4$@mSiO$_2$

For mesoporous with Cu-Fe$_3$O$_4$@mSiO$_2$ catalytic system, Cu and Fe based oxides played important roles in the reaction. In the initial reaction, peroxybenzoic acid was generated by benzaldehyde and oxygen in air. Then, cyclohexanone was attacked by

23

perbenzoic acid to form Criegee adduct according to the common mechanism of B-V oxidation. The reaction could be speed up since the porous structure of Cu-Fe$_3$O$_4$@mSiO$_2$ offered raised numbers of accessible active sites and enhanced mass transfer of reactants and products[35]. This conclusion also could be evidenced with the comparison of mesoporous Cu-Fe$_3$O$_4$/mSiO$_2$ and nonporous N-Cu-Fe$_3$O$_4$/SiO$_2$ with the same copper loading (Fig. 9). From Fig. 9(a), cyclohexanone could be consumed >99% after 6 h and the amounts of peracid species were also higher than those in Fig. 9(b). The consumption of benzaldehyde remained quite low in N-Cu-Fe$_3$O$_4$/SiO$_2$ which also confirmed the low catalytic efficiency of N-Cu-Fe$_3$O$_4$/SiO$_2$. The main difference of mesoporous Cu-Fe$_3$O$_4$/mSiO$_2$ and nonporous N-Cu-Fe$_3$O$_4$/SiO$_2$ catalytic system is the porous structure. The external and internal mass transfer limitations of these two catalytic systems were different. And this only structure difference for the copper and silica supported Fe$_3$O$_4$ microspheres might be responsible for the enhanced mass transfer for the cyclohexanone and related products. The followed scheme by the rearrangement to produce ε-caprolactone and by- product benzoic acid was illustrated in Scheme 1.
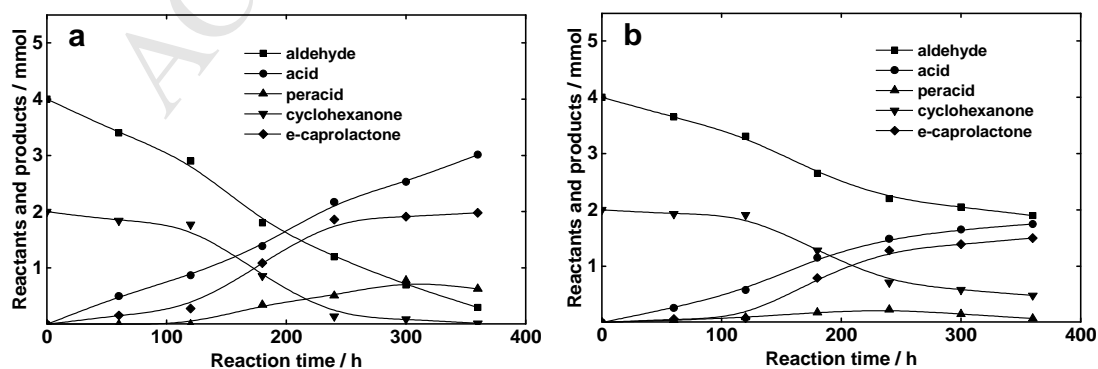

24

Fig. 9. Comparison of mesoporous $Cu-Fe_3O_4@mSiO_2$ (a) and nonporous

$N-Cu-Fe_3O_4/SiO_2$ (b) for the B-V oxidation of cyclohexanone. Reaction conditions:

the catalysts (50 mg), DCE (10 mL), cyclohexanone (2 mmol, 206 uL),

benzaldehyde (4 mmol, 405 uL), air (20 mL/min), 50 °C, reaction time 6 h.

Furthermore, in the mixed ketones, the catalyst still exhibits higher conversion rate

for cyclohexanone (80%) with smaller molecular weight, and the conversion rate of

large molecules, such as acetophenone, is only 33% (Scheme 2). Hence, this catalysts

system could be used as shape selectivity catalysts in aerobic Baeyer-Villiger

oxidations for cyclic ketones with different molecular sizes.
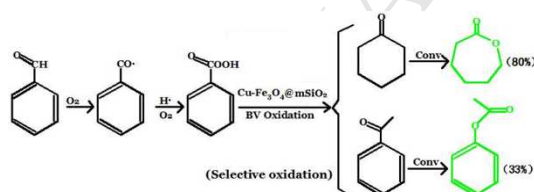
Scheme 2. The shape-selectivity conversion for mixed ketones with

$Cu-Fe_3O_4@mSiO_2$

3. Conclusion

In conclusion, magnetite Cu modified Fe_3O_4 supported mesoporous silica

microspheres ($Cu-Fe_3O_4@mSiO_2$) have been prepared by two step hydrothermal

method. The microspheres possess high surface area, large pore volume, uniform

mesoporous and high magnetization. The catalytic activity of $Cu-Fe_3O_4@mSiO_2$ was

investigated in aerobic Baeyer-Villiger reaction, which superb cyclohexanone

conversion (99.0 %) and selectivity of ε-caprolactone (99.0 %) could be obtained with

benzaldehyde and in air condition. In the presence of mixed ketones, the catalyst still exhibits higher conversion rate for cyclohexanone (80%) with smaller molecular weight, indicating certain shape-selectivity of $Cu-Fe_3O_4@mSiO_2$ for different cyclic ketones. The catalyst could be reused after air calcination with slight loss in catalytic performance for B-V oxidation. The Cu-Fe based oxides in the catalyst activates cyclohexanone and the mesoporous structure could offer enhanced mass transfer for the substrates and products. Additionally, the catalyst could be fast separated from aqueous solution with external magnet after the catalytic reaction. Considering useful magnetic properties, unique mesoporous structure and highly efficient catalytic performance, superparamagnetic mesoporous $Cu-Fe_3O_4@mSiO_2$ microspheres could offer promising applications for aerobic Baeyer-Villiger oxidation of different and mixed cyclic ketones.

4. Experimental section

4.1 Materials

The chemicals used in this work are ethylene glycol, ferric chloride, sodium acetate (NaAC), tetraethyl orthosilicate (TEOS), ethanol, copper nitrate trihydrate (analytical grade, Tianjin Chemical Corp.). Cetyltrimethylammonium bromide (CTAB) was purchased from Sigma-Aldrich. The organic reagents used in the catalytic reaction were supplied from Tianjin Chemical industry. All of the chemicals were used as received without further purification.

4.2 Synthesis

4.2.1 Preparation of Fe₃O₄ particles

Magnetic Fe_3O_4 nanoparticles were synthesized by an improved hydrothermal reaction [39]. Typically, 1.35 g of $FeCl_3 \cdot 6H_2O$ was dissolved into ethylene glycol (40 mL) and heated to 60 °C under stirring for 10 min, followed by the addition of sodium acetate (3.6 g). After stirred vigorously for 30 min, the obtained yellow mixture was transferred to a Teflon-lined stainless steel autoclave, sealed and crystallized at 180 °C for 24 h. When cooled naturally to the ambient temperature, the obtained black production was separated with magnet, washed completely with ethanol several times, and then dried in a vacuum at 60 °C overnight.

4.2.2 Preparation of Cu-Fe₃O₄@mSiO₂ and I-Cu-Fe₃O₄@mSiO₂ microspheres

The $Cu\text{-}Fe_3O_4@mSiO_2$ microspheres were prepared by a directly hydrothermal way. Typically, Fe_3O_4 (100 mg) microspheres were redispersed into a mixed solution in three-neck flask consisting of CTAB (0.3 g). Certain amount of $Cu(NO_3)_2 \cdot 3H_2O$ were dissolved into 80 mL distilled water, ethanol (60 mL) and aqueous ammonia solution (1.1 mL, 28 %). After stirred mechanically for 30 min, TEOS (1.5 mL, 98 %) was introduced dropwise into the mixture and kept stirring for 6 h at 50 °C. Subsequently, the solution was transferred to a PTFE-lined stainless steel autoclave and heated to 100 °C for 12 h. The resulting production was filtered, washed with large amount of water and ethanol, followed by dried at 40 °C for 12 h. Finally, the solid was calcined at 823 K for 6 h with 3 K/min in tubed furnace to remove the template agent. The

obtained productions were denoted as $Cu-Fe_3O_4@mSiO_2$. Without addition of CTAB, the same above nonporous microspheres were prepared and denoted as $N-Cu-Fe_3O_4@SiO_2$. Meanwhile, $Fe_3O_4@mSiO_2$ microspheres were synthesized with same above way without the addition of $Cu(NO_3)_2 \cdot 3H_2O$.

I-$Cu-Fe_3O_4@mSiO_2$ microspheres were prepared in comparison to the materials above by the conventional impregnation method. 100 mg of $Fe_3O_4@mSiO_2$ microspheres were dispersed into ethanol (15 mL). Then $Cu(NO_3)_2 \cdot 3H_2O$ (0.080 g) was added into the above mixture. The solution was stirred until ethanol were evaporated completely, followed by dryness in a vacuum at 60 °C 4 h and 100 °C for 4 h. Then, the obtained materials were calcined at 550 °C for 6 h at air atmosphere to remove CTAB template. The obtained catalyst was denoted as I-$Cu-Fe_3O_4@mSiO_2$.

4.3 Measurements and Characterizations

Powder X-ray diffraction patterns of the samples were determined on a D8 ADVANCE (America) with Cu Kα radiation operating at 40 kV and 40 mA. FT-IR measurements were recorded with Gangdong Fourier Transforms Infrared (FT-IR) spectrometry 650 (China) with KBr pellet technique in the range of 500 ~ 4000 cm^{-1}. Transmission electron microscope (Hitachi H-7650) were used to confirm the morphology and texture of the samples at accelerating voltage of 300 kV. N_2 sorption-desorption isotherms were used to calculated the BET surface area, mesoporous size distribution and the total pore volume. Magnetic studies were carried out through Squid-VSM magnetometer at room temperature. Diffuse reflectance

UV-vis spectra were recorded between 190 ~ 800 nm at room temperature using U-2700 spectrophotometer (Hitachi) with $BaSO_4$ as reflectance sample.

4.4 Catalytic reaction

The catalytic activity of mesoporous silica materials including Cu containing $Fe_3O_4@mSiO_2$ was evaluated with different cyclic ketones. The activity tests were performed in a three-neck flask placed in temperature-controlled oil bath. In a typical synthesis, the reaction mixture consists of catalyst (50 mg), cyclohexanone (2 mmol, 206 uL), benzaldehyde (4 mmol, 0.424 g) and 1,2-dechloroethane (10 mL) was stirred vigorously stirred with magnet and heated to 50 ℃ for 6 h, equipped with a reflux condenser. Air was introduced into the flask continuously at 20 mL/min. The obtained products were centrifuged and analyzed using HP 9790II gas chromatograph equipped with poly-capillary column and hydrogen flame ionization detector. The dodecane was chosen as an internal standard to calculate the conversion of ketones, selectivity of caprolactone and the conversion of aldehydes. The used catalysts were collected with a magnet and filtered, washed with ethanol and dried at 100 ℃ for 6 h and then subjected to the next catalytic cycle.

Conflicts of interest

There are no conflicts to declare.

Acknowledgment

Reference

1 Renz M, Meunier B. *Eur J Org Chem*. 1999;30:737-750.

2 Michelin RA, Sgarbossa P, Scarso A, Strukul G. *Coordin Chem Rev*. 2010; 254:646-660.

3 Jeong EY, Ansari MB, Park SE. *ACS Catal*. 2011;1:855-863.

4 Gusso A, Baccin C, Pinna F, Strukul G. *Organometallics*. 1994;13:3442.

5 Kaneda K, Yamashita T. *Tetrahedron Lett*. 1996;37:4555-4558.

6 Zarrabi S, Mahmoodi NO, Tabatabaeian K, Zanjanchi MA. *Chinese chem lett*. 2009;20:1400-1404.

7 Alam MM, Varala R, Adapa SR. *Synthetic Commun*. 2003;33:3035-3040.

8 Yadav JS, Reddy BVS, Basak AK, Narsaiah AV. *Chem lett*. 2004;35:211-239.

9 Sinhamahapatra A, Sinha A, Pahari SK, Sutradhar N, Bajaj HC, Panda AB. *Catal Sci Technol*. 2012;2:2375-2382.

10 Zhou W, Tian P, Sun FA, He M, Chen Z. *Asian J Org Chem*. 2014;4:33–37.

11 Li J, Le Y, Dai WL, Li H, Fan K. *Catal Commun*. 2008;9:1334-1341.

12 Li YF, Guo MQ, Yin SF, Chen L, Zhou YB, Qiu RH, Au CT. *Carbon*. 2013;5:269-275.

13 Zang J, Ding YJ, Yan L, Wang T, Lu Y, Gong LF. *Catal Commun*. 2014;51:24-28.

14 Nabae Y, Rokubuichi H, Mikuni M, Kuang Y, Hayakawa T, Kakimoto M. *ACS Catal.* 2013;3:230-236.

15 Luo HY, Bui L, Gunther WR, Min E, Románleshkov Y. *ACS Catal.* 2012;2:2695-2699.

16 Corma A, Nemeth LT, Renz M, Valencia S. *Nature.* 2001;412:423-425.

17 Mazzini C, Jacques Lebreton A, Furstoss R. *J Org Chem.* 1996;61:8-9.

18 Corà F, Catlow CRA, *P Roy Soc A Math Phy.* 2012;468:2053-2069.

19 Hara T, Hatakeyama M, Kim A, Ichikuni N, Shimazu S. *Green Chem.* 2012;14:771-777.

20 Li YF, Guo MQ, Yin SF, Chen L, Zhou YB, Qiu RH, Au CT. *Mechanisms and Catalysis.* 2013;109:525-535.

21 Huang S, Li C, Cheng Z, Fan Y, Yang P, Zhang C, Yang K, Lin J. *J Colloid Interf Sci.* 2012;376:312-321.

22 Chen HM, Deng CH, Zhang XM. *Angew Chem Int Edit.* 2010;49:607-611.

23 Yue Q, Li JL, Luo W, Zhang Y, Elzatahry AA, Wang XQ, Wang C, Li W, Cheng XW, Alghamdi A, Abdullah AM, Deng YH, Zhao DY. *J Am Chem Soc.* 2015;137:13282-13289.

24 Liu F, Tian H, He JH. *J Colloid Interf Sci.* 2014;419:68-72.

25 Deng Y, Qi D, Deng C, Zhang X, Zhao D. *J Am Chem Soc*. 2008;130:28-29.

26 Huang XB, Guo WC, Wang G, Yang M, Wang Q, Zhang XX, Feng YH, Shi Z, Li CG. *Mater Chem Phys.* 2012;135:985-990.

27 Velu S, Wang L, Okazaki M, Suzuki K, Tomura S. *Microp Mesop Mat*. 2002;54:113-126.

28 Gomes HT, Selvam P, Dapurkar SE, Figueiredo JL, Faria JL. *Microp Mesop Mat*. 2005;86:287-294.

29 Jeong EY, Ansari MB, Park SE. *ACS Catal*. 2011;1:855-863.

30 Rahman S, Enjamuri N, Gomes R, Bhaumik A, Sen D, Pandey JK,   Mazumdar S, Chowdhury B. *Appl Catal A-Gen*. 2015;505:515-523.

31 Liu F, Tian H, He J. *J Colloid Interf Sci*. 2014;419:68-72.

32 Shi L, Yu TT, Lin S, Lin C. *J Mater Sci*. 2016;51:4942-4951.

33 Chanquía CM, Cánepa AL, Bazán-Aguirre J, Sapag K, Rodríguez-Castellón E, Reyes P, Herrero ER, Casuscelli SG, Eimer GA. *Micropor Mesopor Mat*. 2012;151:2-12.

34 Huo HF, Wu L, Ma JX, Yang HL, Zhang L, Yang YY, Li SW, Li R. *Chemcatchem*. 2016;8:779-786.

35 Wang Y, Zhao H, Li M, Fan J, Zhao G. *Appl. Catal. B*, 2014;147:534-545.

36 Ruiz JR, Jimenez-Sanchidrian C, Llamas R. *Tetrahedron.* 2006;62:11697-11703.

37 Kwan WP, Voelker BM. *Environ Sci Technol.* 2003;37:1150-1158.

38 Cai C, Zhang H, Zhong X, Hou LW. *J Hazard Mater*. 2015;283:70-79.

39 Deng H, Li XL, Peng Q, Wang X, Chen JP, Li YD. *Angew Chem Int Edit*. 2005;44:2782-2785.

Highlights

- Fe-Cu composite core-shell mesoporous silica nanospheres

- Enhanced shape-selectivities for mixed cyclic ketones with mesoporous structures

- High catalytic performance in aerobic Baeyer-Villiger oxidation for Fe-Cu combination

- Easily separation of nanospheres from reaction with superparamagnetic properties